J. Fluid Mech. (1976), *vol.* 76, *part* 3, *pp.* 593–621
Printed in Great Britain

Condensation shocks in nozzle flows

By P. A. BLYTHE AND C. J. SHIH

Center for the Application of Mathematics, Lehigh University,
Bethlehem, Pennsylvania 18015

(Received 16 February 1976)

Supersonic nozzle flows of a condensable vapour are considered in the high activation limit for homogeneous nucleation. Conditions are determined under which the final collapse of the supersaturated state is described by a condensation shock. It is shown that the shock zone is associated with droplet growth: droplet production occurs in a thin layer upstream of the growth region. Some new scaling laws are obtained for the structure of the production layer.

1. Introduction

Condensation effects in expanding flows have been examined in a wide variety of contexts. Their appearance in supersonic wind tunnels, due to the presence of small amounts of water vapour, is well known (Lukasiewicz & Royle 1953). In hypersonic tunnels test section temperatures are often low enough for condensation of the working fluid itself to limit the performance of the facility (Clark 1963). Analyses have been carried out for metal vapours with respect to their possible application in propulsive devices for space vehicles (Hill, Whitting & Demetri 1963). Currently, nozzle flows are being increasingly used as a quantitative tool for the general study of nucleation rates (Andres 1969). Reviews of both the theoretical and the experimental work can be found in Wegener (1969, 1975). Earlier work in this field has been well documented by Wegener & Mack (1958) and Stever (1958).

Figure 1 shows a conventional pressure–temperature diagram for nozzle flows. Reservoir conditions correspond to the vapour state. As the flow expands the initial isentrope crosses the co-existence line at the saturation point x_c. Since the growth rate of the condensed phase is zero at x_c a region of supersaturated flow will exist. For homogeneous or self-nucleation it is often observed that this supersaturated state persists over a significant distance downstream of x_c and, further, that the eventual breakdown of the supersaturated state occurs in a rather abrupt manner. Investigations of this sudden collapse led to the concept of a condensation shock. Strictly, the shock is a narrow region whose structure is defined by the local heat release. Within the collapse zone the growth rate is large. As the position of the collapse moves further downstream, corresponding to smaller growth rates, the condensation zone is of a more diffuse nature (see, for example, figure 5, Hill 1966).

For sufficiently large growth rates the collapse occurs close to the initial saturation point. Apart from a thin transition layer near x_c, the bulk of the flow

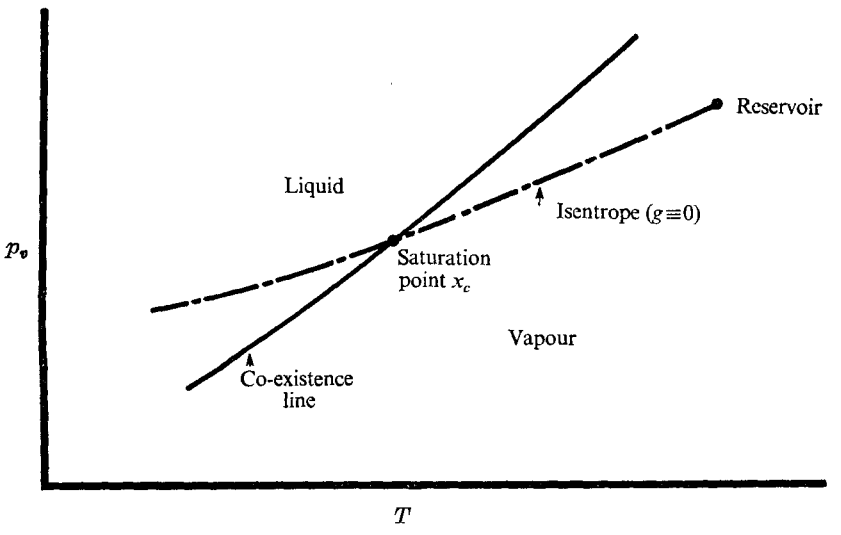

FIGURE 1. p_v, T curve (schematic).

is then governed by the saturated equilibrium relations. Data for air suggest that, in some cases, near-equilibrium collapses of this kind may be due to heterogeneous nucleation (Daum & Gyarmathy 1968).

Only homogeneous nucleation is considered in this paper. It is convenient to introduce both a growth parameter λ (ratio of a flow time to a growth time) and a production or nucleation parameter K. The latter parameter is proportional to the inverse of a non-dimensional activation energy required for the formation of droplets of critical size. $K \ll 1$ is equivalent to low production rates or high activation energies. Although the growth parameter is controlled in part by the nozzle geometry, the nucleation parameter, for any given vapour, is a function only of the reservoir conditions.

Experimental observations of condensation shocks should occur in flows for which $\lambda \gg 1$ and $K \ll 1$. Calculations for various vapours (figure 2) indicate that there is indeed a broad range of reservoir conditions over which $K \ll 1$. Flows with $\lambda \gg 1$ will always arise if the expansion rate is sufficiently slow. The present paper is concerned with quasi-one-dimensional nozzle flows (§2) in the limit $\lambda \to \infty$, $K \to 0$. In particular, the paper discusses the existence, position and structure of condensation shocks. Classical shock analyses, which are concerned simply with conservation laws, do not provide information on these points (Wegener & Mack 1958).

As a means of ordering the double limit it is convenient to introduce an effective onset point for the nucleation process. Rate laws governing the production and growth of the condensation nuclei (see §3) indicate that homogeneous nucleation is dominated by an exponential dependence on the activation function B. This function is proportional to the local activation energy and its variation with distance x through the nozzle is shown in figure 3. For small K, the production rate exhibits a marked peak near the minimum at x_k which provides a satis-

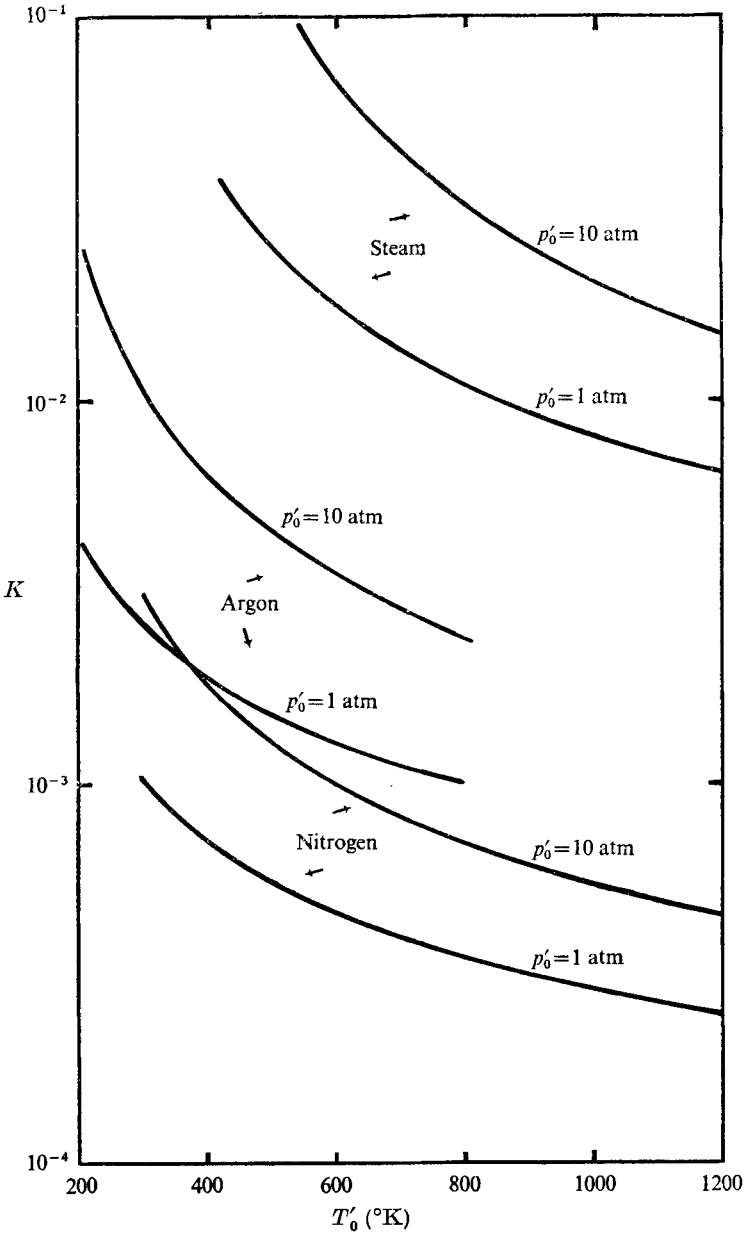

FIGURE 2. The nucleation parameter for steam, argon and nitrogen.

factory definition for the onset point (§4). The limit $\lambda \to \infty$, $K \to 0$ is now replaced by $K \to 0$, $x_k - x_c = O(1)$.

It is important to note that, even if the local activation energy is evaluated completely from the supersaturated solution, the corresponding function B_f, which is a lower bound for B, still has a minimum at some point $x_m \geqslant x_k$ (see figure 3). When x_k is not close to x_m it is shown in §§5–7 that the final collapse of

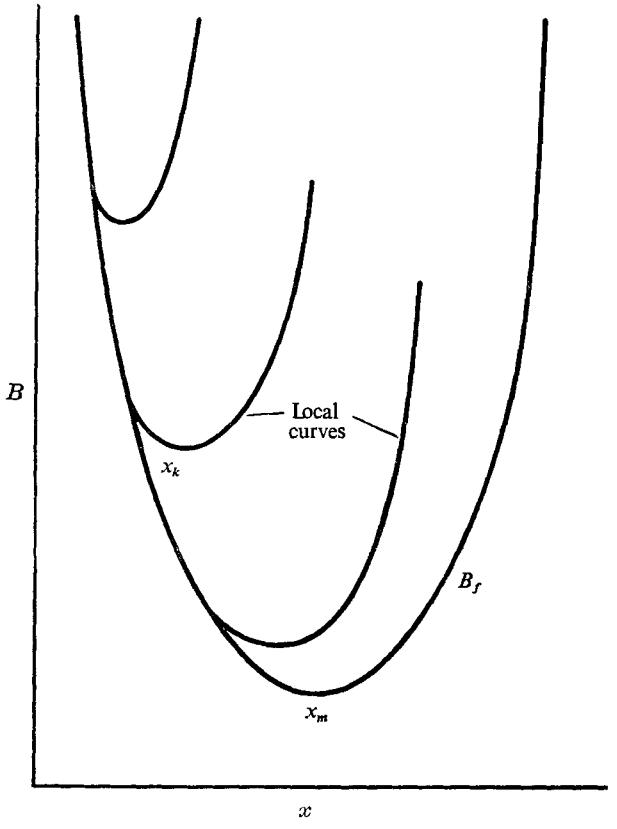

FIGURE 3. Frozen and local behaviour of the activation function B.

the supersaturated state is governed by a condensation shock. More precisely, the collapse is found to have a two-layer structure in which the first layer is dominated by droplet production. Major growth occurs in the second layer or shock zone where nucleation is no longer important. Both layers are narrow in extent but the area variation cannot be neglected in the nucleation zone. Within the nucleation region, however, the rate equation can be reduced to a parameter-free similarity form (§5). This scaling law should be of practical interest.

As $x_k \to x_m$, or equivalently as λ decreases at fixed K, the collapse becomes less sharp. In this case the final approach towards a saturated state is not necessarily described by a condensation shock. Simplifications do still occur within the nucleation zone, where it is now found that the rate equation can be reduced to a form depending on only a single parameter. A detailed discussion of the structure is given in §§8 and 9.

Although the droplet growth law (§3) implies that the downstream limit of the shock solution should be defined by a saturated state, it is well known that such states are not always admissible since the heat release due to condensation can lead to thermal choking (Wegener & Mack 1958). A combined analysis of the growth law and of the shock relations (§7) shows that choking is possible only

if the initial saturation point occurs upstream of the nozzle throat. This latter condition is apparently not well known.

The principal results obtained in this paper are summarized in § 10.

2. Quasi-one-dimensional flows

The general problem considered concerns nozzle flows of a mixture of a condensable vapour and an inert carrier gas. Reservoir conditions are such that the initial point in the vapour pressure–temperature (p_v', T') plane lies beneath the co-existence line (see figure 1). Only those flows for which the initial isentrope crosses the co-existence line are of interest. Downstream of this intersection local equilibrium conditions correspond to saturated states which are governed by the Clausius–Clapeyron equation

$$dp_s'/dT' = L'\rho_v'/T', \tag{2.1}$$

where the volume occupied by the liquid phase has been neglected. p_s' is the saturated vapour pressure, ρ_v' is the vapour density and L' is the latent heat of vaporization. A brief description of the equilibrium solution is given in appendix B. Since the condensation (nucleation) rate is finite, the solution, in general, does not follow the saturation line and a region of supersaturated flow exists. It is the prediction and the structure of the collapse of this supersaturated state which is the central concern of the present paper.

The conservation laws for quasi-one-dimensional flows are taken to have the standard form given in Wegener & Mack (1958), where a detailed discussion of the relevant assumptions can be found. Treating the vapour phase of each component of the mixture as a perfect gas, balance of mass, momentum and energy gives

$$\rho u A = m, \tag{2.2}$$

$$\rho u\, du/dx = -dp/dx, \tag{2.3}$$

$$c_{p0}T + \tfrac{1}{2}u^2 - Lg = c_{p0} + \tfrac{1}{2}u_c^2 = c_{p0}T_0, \tag{2.4}$$

where the suffix 0 corresponds to reservoir conditions and the suffix c to conditions at the saturation point. ρ is the density of the mixture, p is the pressure, T is the temperature, g is a weighted mass fraction, c_p is the specific heat at constant pressure for the mixture, L is the latent heat, x measures distance through the nozzle ($x = 0$ at the throat), $A(x)$ is the local cross-sectional area and m is the mass flow rate. All dependent variables are now normalized with respect to conditions at the saturation point; x is normalized with respect to the nozzle throat height (see appendix A). At $x = x_c$, $p = \rho = T = 1$ and $g = 0$.

The weighted mass fraction g is related to the actual mass fraction g' by

$$g = (\mu_0/\mu_v)\, Hg', \tag{2.5}$$

where

$$H = \mu_v L_c'/\mathscr{R}T_c'. \tag{2.6}$$

$\mathscr{R}$ is the gas constant, μ_0 is the molecular weight of the mixture in the reservoir and μ_v is the molecular weight of the vapour. In terms of these variables the

equation of state for the mixture becomes

$$p = \rho(1 - H^{-1}g)\,T. \tag{2.7}$$

Relationships between the partial pressures etc. are listed in appendix A.

From (2.1), assuming $L = L(T)$ (see §3), it follows that the normalized saturation pressure is given by

$$p_s = \exp\left[H\int_1^T L(\tau)\,\tau^{-2}d\tau\right], \tag{2.8a}$$

which simplifies to

$$p_s = \exp\left[-H(T^{-1} - 1)\right] \tag{2.8b}$$

if L is constant. Similarly, the saturation temperature T_s corresponding to the local vapour pressure is defined implicitly from (2.8) by

$$\int_1^{T_s} L(\tau)\,\tau^{-2}d\tau = H^{-1}\ln(p_v), \tag{2.9}$$

with a subsequent simplification if L is constant.

3. The rate equation

For homogeneous nucleation, condensation nuclei of critical size are formed by random molecular processes. If $m_r'(x', \xi')$ is the mass at x' of a droplet of radius r' which originated at ξ' and if $J'(\xi')$ is the rate of production per unit volume of droplets of critical size then

$$g' = \frac{1}{m'}\int_{-\infty}^{x'} m_r'(x', \xi')\,J'(\xi')\,A'(\xi')\,d\xi'. \tag{3.1}$$

The droplet growth rate, which determines m_r', depends on the ratio of the droplet size to the mean free path. Operating conditions in supersonic wind tunnels are usually such that a molecular growth law is appropriate. Strictly it is necessary to consider both the mass and the energy balance for the droplet but it has been found (Buhler 1952; Hill 1966) that in many cases the energy balance can be replaced by a quasi-equilibrium assumption in which the droplet temperature T_D is defined in terms of local conditions. The approximation that T_D is also independent of the droplet size is often made (Hill 1966) and will be adopted here. Consequently, in dimensionless form,

$$T_D = T_D(p_v, T, g), \tag{3.2}$$

which for a pure vapour reduces to $T_D = T_D(p_v, T)$. Expressions for T_D in the case of gas–vapour mixtures can be obtained from the discussion in Hill (1966). No particular choice of the function $T_D(p_v, T, g)$ is necessary for the general analysis given in this paper but it is important to note that on an equilibrium curve

$$T = T_D = T_s \tag{3.3}$$

for all g. T_s is the saturation temperature defined by (2.9). Consistent with the size-independent assumption on T_D, it is necessary to take

$$L = L(T), \tag{3.4}$$

and to neglect any dependence on the droplet radius. Detailed calculations can be found in Wegener & Parlange (1967).

In normalized form, the molecular growth law for the droplet radius r is

$$dr/dx = \lambda F(p_v, T, g)\,[T_D - T], \tag{3.5}$$

where λ is the growth or rate parameter, which corresponds to a characteristic ratio of a flow time to a droplet growth time (appendix A). This paper is concerned throughout with the limit $\lambda \gg 1$. The rate function F is inversely proportional to the speed $u(T, g)$ [see (2.4)]. Other than the requirement that F be differentiable with respect to any of its arguments no detailed assumptions on its general behaviour are necessary. At the saturation point $F(1, 1, 0) = 1$. From the size-independent assumption it follows that the right-hand side of (5.3) is defined solely in terms of the thermodynamic variables p_v, T and g.

Various expressions for the droplet production rate J' have been derived. Reviews of current theories can be found in Wegener (1969) and Andres (1969). These theories all lead to expressions of the form

$$J' = S'\Sigma(p_v, T) \exp\{-K^{-1}B(p_v, T)\} = S'J(p_v, T; K), \tag{3.6}$$

where B is proportional to the activation energy associated with the formation of droplets of critical size. K is referred to as the nucleation parameter. It is defined implicitly by the particular choice of the function $B(p_v, T)$. Classical theories predict that

$$B = \mathscr{B}(p_v, T)\,(\ln s)^{-2}, \tag{3.7}$$

where

$$s = p_v/p_s \tag{3.8}$$

is the saturation ratio and the normalization is such that $\mathscr{B}(1, 1) = 1$. Some calculations for K were shown in figure 2. The thermodynamic data were obtained from the International Critical Tables and from Wegener (1969); the nucleation rate was defined by the result due to Volmer (1939). Similar results, in which $K \ll 1$ over a broad range of reservoir conditions, appear to hold for many other vapours of practical interest. Only flows with $K \ll 1$ are considered in this paper.

Although there has been some discussion concerning the pre-exponential factor in (3.6) (Lothe & Pound 1962; Andres 1969) this question will not affect the qualitative conclusions of the present analysis since no specific choice of the function $\Sigma(p_v, T)$ need be made. At the saturation point $\Sigma(1, 1) = 1$.

Finally, using these normalized variables, the rate equation (3.1) becomes

$$g = \lambda^3 \int_{-\infty}^{x} \mathscr{M}(x, \xi)\, J(\xi)\, A(\xi)\, d\xi, \tag{3.9}$$

where, from (3.5), $$\mathscr{M}(x, \xi) = \left[\int_{\xi}^{x} F(\eta)\,[T_D(\eta) - T(\eta)]\, d\eta\right]^3. \tag{3.10}$$

It has been assumed that the initial (critical) droplet radius can be neglected; this assumption is consistent with the size-independent approximation made earlier. Some numerical calculations can be found in Wegener & Mack (1958).

4. Initial growth

Near the saturation point x_c, where B is unbounded, g is exponentially small. If $K \ll 1$ it can be expected that a supersaturated state will persist for some distance downstream of x_c even though the growth parameter $\lambda \gg 1$. Here the double limit $\lambda \to \infty$, $K \to 0$ is ordered such that the collapse of the supersaturated state occurs at a finite distance downstream of x_c. Over the interval $x_k > x \geqslant x_c$, where x_k is the effective onset point [see (4.10)], the first approximation to the solution is governed by the frozen relations ($g \equiv 0$)

$$p_f = T_f^{\gamma/(\gamma-1)}, \quad \rho_f = T_f^{1/(\gamma-1)}, \quad u_f^2 = \frac{2\gamma}{\gamma-1}(T_0 - T_f), \tag{4.1}$$

with

$$\gamma = c_{p0}/(c_{p0}-1). \tag{4.2}$$

This system is completed by the continuity equation (2.2). If the saturation point x_c lies downstream of the nozzle throat the mass flow rate is defined by the condensate-free value

$$m_f = \gamma^{\frac{1}{2}} \left(\frac{2T_0}{\gamma+1}\right)^{\frac{1}{2}(\gamma+1)/(\gamma-1)}. \tag{4.3}$$

Even if x_c lies upstream of the throat, the mass flow is still determined to a first approximation by (4.3) if the onset point x_k occurs downstream of the throat. The analysis in this paper is initially restricted to flows which are supersonic at x_k.

From (3.6) and (3.9) it can be shown that the initial growth of the condensate mass fraction is given by

$$g = \lambda^3 \int_1^x \mathscr{M}_f(x,\xi)\, \Sigma_f(\xi)\, A(\xi) \exp\{-K^{-1} B_f(\xi)\}\, d\xi [1 + O(g/K)], \tag{4.4}$$

where the suffix f denotes evaluation from the condensate-free solution. It is important to observe that in (4.4) the error term, which represents the coupling between the rate and flow equations, is $O(g/K)$.

The growth defined by (4.4) depends strongly on the behaviour of the function $B_f(x)$. Standard expressions for the activation energy lead to curves of the type that were shown in figure 3. In particular, (3.7) implies that as $x \to x_c$

$$B_f \sim (x - x_c)^{-2}, \tag{4.5}$$

apart from some constant factor. As $x \to \infty$ ($A \to \infty$) the classical theory (Volmer 1939) yields

$$B_f \sim A^{4(\gamma-1)}, \tag{4.6}$$

again apart from a constant factor. For the general analysis, with $x_k > x_c$, it is not necessary to use the specific results (4.5) and (4.6), but it is required that B_f have the characteristic shape given in figure 3 with a single minimum at $x = x_m$.

As $K \to 0$ the integrand in (4.4) is of steepest-descent type with a turning point at x_m. However, the error term in (4.4) can become important upstream of x_m. In this case the coupling limits the droplet production and leads to a local minimum of the activation function $B(p_v, T)$ (see figure 3). Although g is still small in this region, it is found that the coupled turning point is closely associated with the collapse point x_k (§5). It is necessary to distinguish between flows for which

x_k lies upstream of x_m and flows for which $x_k \sim x_m$. Only the former case is considered in this section. Results for the limit $x_k \sim x_m$ are discussed in §§ 8 and 9.

Neglecting the factor $O(g/K)$, it can be shown from (4.4) that upstream of x_m

$$g \sim 6\lambda^3 K^4 \Omega_f^3(x)\, \Sigma_f(x)\, A(x)\, (dB_f/dx)^{-4} \exp\{-K^{-1}B_f(x)\}\,[1+O(K)], \quad (4.7)$$

where
$$\Omega_f = F_f(T_{Df} - T_f), \quad (4.8)$$

provided that
$$K^{-\frac{1}{2}}|dB_f/dx| \gg 1. \quad (4.9)$$

Clearly, from (4.4), this initial growth law will remain valid, $x < x_m$, only if $g = o(K)$. If λ is sufficiently large it can be seen that this restriction will be violated at a finite distance upstream of x_m. The point x_k characterizing the position of this onset region, where the coupling between the rate and flow equation can no longer be neglected, is defined implicitly by

$$g(x_k)/K \sim D(x_k) = 6\lambda^3 K^3 \Omega_k^3 \Sigma_k A_k (dB_f/dx)_k^{-4} \exp\{-K^{-1}B_k\} = 1 \quad (4.10)$$

with $\Omega_k = \Omega_f(x_k)$, etc.

Onset criteria have been discussed extensively in the literature (Wegener 1969; Wegener & Mack 1958) and it is of interest to note that Oswatitsch (1941), using qualitative arguments, obtained a result similar in form to (4.10). In addigion to the exponential factor, Oswatitsch's criterion included the term $(dT/dx)^{-4}$. A similar term $(dB_f/dx)^{-4}$ arises in (4.10) (see also Daum & Gyarmathy 1968). The point x_k, defined by (4.10), is probably best referred to as a relative onset point since the critical value of g is measured with respect to the parameter K. Near x_k the flow variables are influenced, even to a first approximation, by the heat release due to condensation. Conventional definitions of the onset point often correspond to the use of some absolute value of the condensation fraction or, at least, to the use of some practical indication, such as static pressure measurements, of the departure from an isentropic state. Analysis of the subsequent growth of the mass fraction (§§ 5 and 6) shows that in the present limit these definitions all predict collapse points which lie close to that given by (4.10).

From (4.10) the parameters λ and K can now be replaced by x_k and K. The appropriate limit is defined by $K \to 0$ with $x_k\,(> x_c) = O(1)$. For given reservoir conditions the nucleation parameter K is fixed but the growth parameter λ depends on the nozzle geometry. Although in general $x_k < x_m$, flows in which $x_k \sim x_m$ can arise from practical situations: this limit will always ultimately occur as λ decreases (rapid expansions) and is discussed in §§ 8 and 9. Conversely, for very slow expansions ($\lambda \to \infty$) $x_k \to x_c$. A brief discussion of this latter limit, in which the bulk of the collapse occurs close to the saturation point, is given at the end of § 7 for $K \ll 1$ (see also Shih 1972). Experimental data confirm that both situations, i.e. $x_k > x_c$ and $x_k \sim x_c$, are of practical significance.

5. The nucleation zone

If x_k does not lie close to either x_c or x_m, appropriate asymptotic expansions in the neighbourhood of x_k are

$$g = Kg_1(\phi_1) + \ldots, \quad (5.1)$$

$$T = T_k + KT_1(\phi_1) + \ldots, \quad (5.2)$$

etc., where $$\phi_1 = K^{-1}(x - x_k). \tag{5.3}$$

These expansions are compatible with the limiting behaviour, $x \to x_k$, of the initial growth law (4.7). Substitution into the conservation equations (2.2)–(2.4), together with the equation of state (2.7), gives

$$(M_k^2 - 1)\, T_1/T_k = -(\gamma - 1)\, M_k^2 A_{1k} \phi_1 + (\gamma - 1)\{M_k^2 - \gamma^{-1} - H_k^{-1} M_k^2\}\, L_k g_1/T_k, \tag{5.4}$$

where $$A_{1k} = \left\{\frac{1}{A}\frac{dA}{dx}\right\}_k, \tag{5.5}$$

$$H_k = HL_k/T_k = \mu_v L_k'/\mathscr{R} T_k', \tag{5.6}$$

and $M_k\ (> 1)$ is the Mach number based on the frozen sound speed. Similar results hold for the remaining dependent variables. The temperature variation is now influenced to first order by the heat release due to condensation: the terms on the right-hand side of (5.4) are associated respectively with the temperature decrease due to the nozzle expansion and with the temperature increase due to the onset of condensation.

In this region the rate equation (3.9) becomes

$$g_1 = \tfrac{1}{6} a^4 \int_{-\infty}^{\phi_1} (\phi_1 - \psi_1)^3 \exp\{a\psi_1 - b g_1(\psi_1)\}\, d\psi_1, \tag{5.7}$$

where use has been made of (5.4) and of the corresponding results for the other dependent variables. The constants a and b are defined by

$$a = -\left(\frac{dB_f}{dx}\right)_k = \frac{M_k^2 A_{1k}}{M_k^2 - 1}\left[(\gamma - 1)\left(T\frac{\partial B}{\partial T}\right)_k + \gamma\left(p_v \frac{\partial B}{\partial p_v}\right)_k\right], \tag{5.8}$$

$$b = b_{Tk}\left(T\frac{\partial B}{\partial T}\right)_k + b_{vk}\left(p_v \frac{\partial B}{\partial p_v}\right)_k, \tag{5.9}$$

with $$b_{Tk} = \frac{(\gamma - 1)\{M_k^2 - \gamma^{-1} - H_k^{-1} M_k^2\}}{T_k(M_k^2 - 1)} \tag{5.10}$$

and $$b_{vk} = \frac{(\gamma - 1) M_k^2 - H_k^{-1}\{\gamma M_k^2 + (1 - \omega_0)\,\omega_0^{-1}\mu_v \mu_0^{-1}(M_k^2 - 1)\}}{T_k(M_k^2 - 1)} \tag{5.11}$$

Since $dB_f/dx < 0\,(x < x_m)$, a is positive. For standard models (Andres 1969) $\partial B/\partial p_v < 0$ and it follows, for $M_k > 1$, that b is also positive.

The scaling transformation

$$g_1 = b^{-1}\hat{g}, \quad \phi_1 = a^{-1}\hat{\phi}, \tag{5.12}$$

together with the change of origin

$$\hat{\phi} = \phi - \ln b, \tag{5.13}$$

reduces (5.7) to the canonical parameter-free form

$$\hat{g}(\phi) = \frac{1}{6}\int_{-\infty}^{\phi} (\phi - \psi)^3 \exp\{\psi - \hat{g}(\psi)\}\, d\psi. \tag{5.14}$$

From (5.14) it appears that within this zone both droplet production and droplet growth are important, though the characteristic feature of the region is the rapid

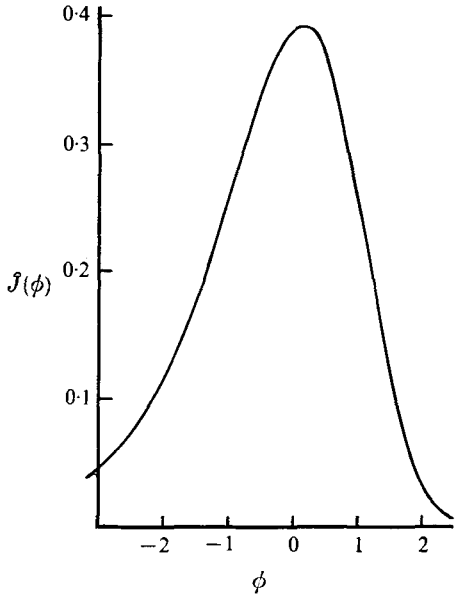

FIGURE 4. The droplet production rate.

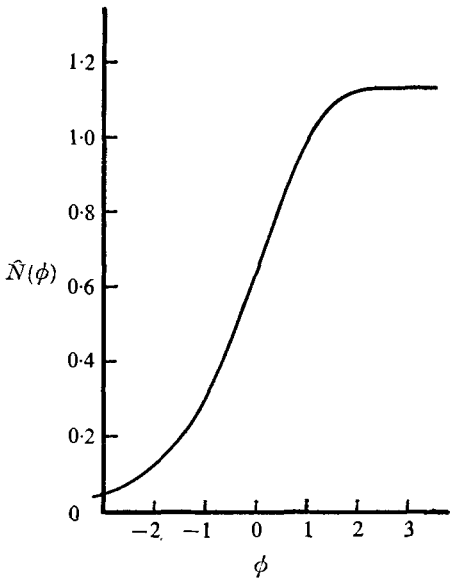

FIGURE 5. The droplet number density.

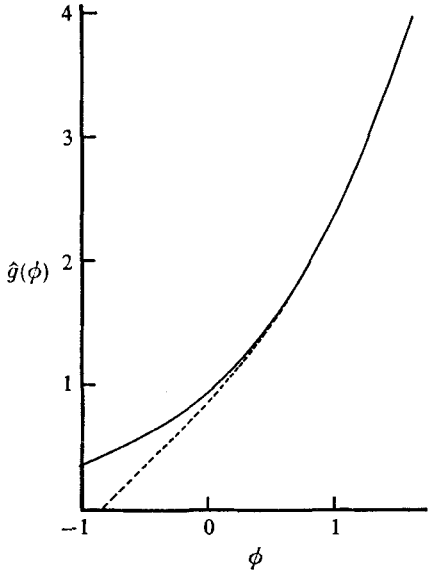

FIGURE 6. Droplet growth. ——, exact solution; – – – –, asymptotic solution (5.18).

increase, and subsequent decay, of the local nucleation rate. This production term is represented by

$$\hat{J}(\phi) = \exp\{\phi - \hat{g}(\phi)\}, \tag{5.15}$$

and a corresponding droplet number density is defined by

$$\hat{N}(\phi) = \int_{-\infty}^{\phi} \hat{J}(s)\, ds. \tag{5.16}$$

A modified predictor–corrector technique was used to obtain the numerical solution of (5.14). The results are shown in figures 4–6. From figure 4 it can be

a_3	a_2	a_1	a_0
0·1883	0·0740	0·3624	0·8566

TABLE 1. The coefficients a_r

seen that the nucleation rate decays rapidly downstream of the present zone and is essentially zero for $\phi > 2$. An appropriate measure of the total number of droplets produced is (figure 5)

$$\hat{N}(\infty) = 1{\cdot}130. \tag{5.17}$$

As $\phi \to \infty$, (5.14) implies that

$$\hat{g} \sim a_3\phi^3 + a_2\phi^2 + a_1\phi + a_0 + o(1), \tag{5.18}$$

where the coefficients a_r, which are defined by

$$a_r = \tfrac{1}{6}\{(-1)^r {}_3C_r\} \int_{-\infty}^{\infty} \psi^r \hat{J}(\psi)\, d\psi, \tag{5.19}$$

are listed in table 1. Figure 6 shows the solution for the mass fraction $\hat{g}$ together with the asymptotic law (5.18). This cubic growth, which corresponds to the droplet radius increasing linearly with distance, obviously cannot persist and must eventially be limited by a return towards a saturated state.

6. Droplet growth

Downstream of the nucleation zone the production rate is exponentially small and the condensation process is dominated by droplet growth. Before discussing the detailed structure of the growth region it is convenient to rewrite the basic rate equation (3.9) in an alternative form using a normalized droplet radius

$$R(x;K) = \int_{\hat{x}_k}^{x} \frac{\Omega(\xi;K)}{\Omega_k}\, d\xi, \tag{6.1}$$

where

$$\Omega(x;K) = F(T_D - T). \tag{6.2}$$

The growth of R is measured from

$$\hat{x}_k = x_k - Ka^{-1} \ln b, \tag{6.3}$$

which corresponds to the origin defined by the transformation (5.13). From (6.1), (3.9) and (3.10) it follows that

$$g(x;K) = \frac{a^4}{6K^3} \sum_{r=0}^{3} (-1)^r {}_3C_r [R(x;K)]^{3-r} I_r(x;K), \tag{6.4}$$

with

$$I_r(x;K) = \int_{x_c}^{x} [R(\xi;K)]^r \frac{\Sigma(\xi;K)}{\Sigma_k} \frac{A(\xi)}{A_k} \exp\{-K^{-1}[B(\xi;K) - B_k]\}\, d\xi. \tag{6.5}$$

Outside the nucleation zone the integrand in (6.5) is exponentially small. It is straightforward to show from the solution given in § 5 that for $x > x_k$ $(x - x_k \gg K)$

$$I_r(x;K) = I_r(\infty;K), \tag{6.6}$$

neglecting exponentially small terms. Further

$$I_r(\infty; K) = Ka^{-1}b^{-1}\int_{-\infty}^{\infty} \phi^r \exp[\phi - \hat{g}(\phi)]\, d\phi[1 + O(K)]. \tag{6.7}$$

Substitution into (6.4) gives

$$g(x; K) = \frac{a}{b}\left(\frac{K}{a}\right)^{-2}\left[\mathscr{A}_3 R^3 + \frac{K}{a}\mathscr{A}_2 R^2 + \left(\frac{K}{a}\right)^2 \mathscr{A}_1 R + \left(\frac{K}{a}\right)^3 \mathscr{A}_0\right] \tag{6.8}$$

with $$\mathscr{A}_{3-r} = \frac{(-1)^r}{6}\,{}_3C_r\left(\frac{K}{a}\right)^{-(r+1)} bI_r(\infty; K) = a_{3-r}[1 + O(K)], \tag{6.9}$$

where a_r is defined by (5.19) (see table 1). Equation (6.8) is an expansion in terms of the local radius and should be compared with (5.18), which is the initial form of this expansion. It is apparent, at least for the leading terms, that in the growth region the mass fraction is independent of the precise origin of the nuclei.

The growth law (6.8) is appropriate downstream of the production zone. Direct inspection of the equations suggests that the nucleation solution will fail when $g = O(1)$ or, equivalently, when $x - x_k = O(K^{\frac{2}{3}})$. (The width of the nucleation zone is $O(K)$.) Within the growth region suitable independent and dependent variables are

$$\chi = l^{-1}K^{-\frac{2}{3}}(x - \hat{x}_k), \quad \bar{R}(\chi; K) = l^{-1}K^{-\frac{2}{3}}R(x; K), \tag{6.10}$$

where $$\bar{R}(\chi; K) = \int_0^{\chi} \bar{\Omega}(s; K)\, ds, \tag{6.11}$$

with $$\bar{\Omega}(\chi; K) = \Omega_k^{-1}\Omega(x; K). \tag{6.12}$$

Inclusion of the factor $$l = a^{-1}(ba_3^{-1})^{\frac{1}{3}} \tag{6.13}$$

in (6.10) leads to some simplification in the subsequent relationships [see (6.15)]. The remaining dependent variables are defined by

$$g(x; K) = \bar{g}(\chi; K), \quad T(x; K) = \bar{T}(\chi; K), \tag{6.14}$$

etc. In the growth region, where $\chi = O(1)$, barred variables are $O(1)$.

Substitution in (6.8) gives

$$\bar{g}(\chi; K) = \bar{R}^3 + a_2 a_3^{-\frac{2}{3}}(Kb^{-1})^{\frac{1}{3}}\bar{R}^2 + a_2 a_3^{-\frac{1}{3}}(Kb^{-1})^{\frac{2}{3}}\bar{R} + O(K). \tag{6.15}$$

Since the a_r are known (table 1) it is clear that, correct to $O(K^{\frac{2}{3}})$, $\bar{g}$ depends only on $\bar{R}$ and the single parameter Kb^{-1}. From (6.11) the integral form of the rate equation is now equivalent to the first-order differential equation

$$d\bar{R}/d\chi = \bar{\Omega}(\chi; K), \tag{6.16}$$

with $$\bar{R}(0; K) = 0. \tag{6.17}$$

In general, $\bar{\Omega} = \bar{\Omega}(\bar{p}_v, \bar{T}, \bar{g})$. $\bar{p}_v$ and $\bar{T}$ are determined as functions of $\bar{g}$ from the local solution of the conservation equations (§7).

Appropriate asymptotic expansions in the growth region are of the form

$$\bar{g}(\chi; K) = \bar{g}_0(\chi) + K^{\frac{1}{3}}\bar{g}_1(\chi) + \ldots, \tag{6.18}$$

etc. It follows from (6.10), however, that the effect of the local area variation is $O(K^{\frac{2}{3}})$. Consequently, the conservation relations reduce to the standard one-dimensional form even if terms $O(K^{\frac{1}{3}})$ are included (§7). Such terms are easily retained in the analysis by introducing the transformation

$$\bar{S}(\chi; K) = \bar{R}(\chi; K) + \tfrac{1}{3}a_2 a_3^{-\frac{2}{3}}(Kb^{-1})^{\frac{1}{3}}. \tag{6.19}$$

Equation (6.15) then becomes

$$\bar{g}(\chi; K) = S^3(\chi; K) + O(K^{\frac{2}{3}}), \tag{6.20}$$

with, from (6.16),

$$d\bar{S}/d\chi = \bar{\Omega}(\chi; K), \tag{6.21}$$

where, from (6.17),

$$\bar{S}(0; K) = \tfrac{1}{3}a_2 a_3^{-\frac{2}{3}}(Kb^{-1})^{\frac{1}{3}} \approx 0{\cdot}2253(Kb^{-1})^{\frac{1}{3}}, \tag{6.22}$$

correct to $O(K^{\frac{1}{3}})$.

From the results of this section, and those of §5, it can be seen that the collapse of the supersaturated state is governed by two distinct regions, both of which lie close to the onset point x_k. The nucleation zone, whose width is $O(K)$, acts as a precursor for the subsequent growth zone of width $O(K^{\frac{2}{3}})$. In this latter zone the rate equation reduces to the simple relaxation form (6.21). The two-zone structure is in qualitative agreement with much of the experimental data and with the results of some numerical solutions of the full equations (see, for example, Clark 1963; Griffin & Sherman 1965; Wegener, Clumpner & Wu 1972). A detailed analysis of the growth region is given in §7.

7. Condensation shocks

Substitution of the expansion (6.14) into the conservation relations (2.2)–(2.4) shows that within the growth zone, correct to $O(K^{\frac{2}{3}})$,

$$\left.\begin{aligned} \bar{\rho}\,\bar{u} &= \rho_k u_k, \\ \bar{p} + \bar{\rho}\,\bar{u}^2 &= p_k + \rho_k u_k^2, \\ c_{p0}\bar{T} + \tfrac{1}{2}\bar{u}^2 - \bar{L}\bar{g} &= c_{p0}T_k + \tfrac{1}{2}u_k^2, \end{aligned}\right\} \tag{7.1}$$

where the right-hand side follows from matching with the upstream nucleation solution. These one-dimensional relations (the local area variation is $O(K^{\frac{2}{3}})$) govern the structure of what is usually termed a condensation shock (Wegener & Mack 1958): the dominant physical mechanism is the heat release due to condensation. This system is completed by the rate law (6.21), together with (6.20), and the equation of state

$$\bar{p} = \bar{\rho}(1 - H^{-1}\bar{g})\,\bar{T}. \tag{7.2}$$

Most models of the shock structure neglect the temperature variation of the latent heat ($\bar{L} = 1$). It is often further assumed that $H \gg 1$. In this latter limit the equation of state reduces to the perfect-gas law

$$\bar{p} = \bar{\rho}\bar{T}. \tag{7.3}$$

The conservation relations remain unchanged in form and, with $\bar{L} = 1$, are equivalent to the classical Rayleigh-line relations governing the flow of a perfect

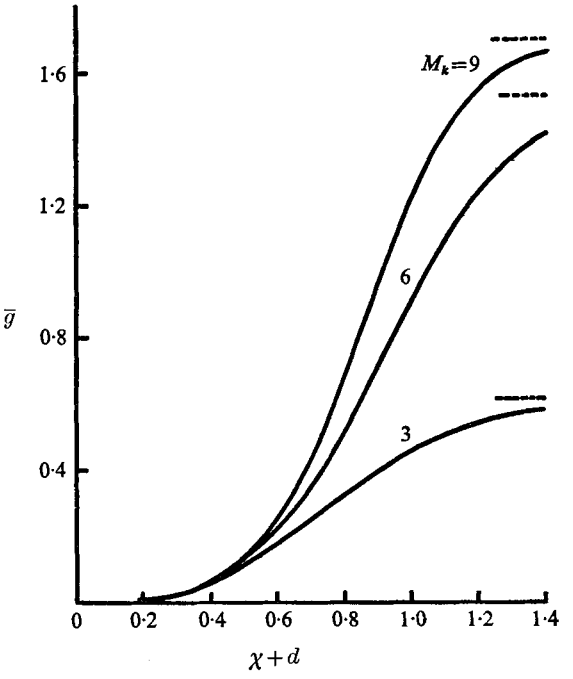

FIGURE 7. Particular examples for the shock structure.
$T_0 = 2$, $\omega_0 = 1$, $\gamma = 1{\cdot}4$, $H = 20$.

gas with heat addition (Shapiro 1953). However, omission of the term $H^{-1}\bar{g}$ in (7.2) can lead to significant errors at high Mach numbers. It will be retained in the present discussion.

Formal integration of the rate equation (6.21) gives

$$\chi+d = \int_0^S \frac{d\sigma}{\bar{\Omega}(\sigma)}. \tag{7.4}$$

For a given growth function $\bar{\Omega}$ is evaluated as a function of $\bar{g}$, and hence of $\bar{S}$, from the solution of the conservation relations. The constant d is determined from the initial condition (6.22). It follows that, correct to $O(K^{\frac{1}{3}})$,

$$d = \tfrac{1}{3}a_2 a_3^{-\frac{2}{3}}(Kb^{-1})^{\frac{1}{3}}. \tag{7.5}$$

Some calculations for a simple model are shown in figure 7, where it was assumed that $T_D = T_s$ (Oswatitsch 1942; Hill 1966) and that $\bar{L} = 1$. These calculations were carried out for a pure vapour ($\omega_0 = 1$) using the growth function

$$F = u_c u^{-1}\rho_v T^{\frac{1}{2}} \tag{7.6}$$

(Wegener & Mack 1958).

For the examples shown in figure 7 the downstream limit of the shock solution corresponds to a saturated state. It might appear from the rate equation that the end state will always be defined by a saturated equilibrium point at which $T = T_D = T_s$. However, it is well known that for flows of this type there is a critical heat addition above which the flow is thermally choked. At choking, the

local Mach number based on the frozen sound speed a_f is unity. a_f is defined by

$$a_f^2 = \left[\frac{\gamma-(\gamma-1)\,g\,dL/dT}{1+(\gamma-1)\,H^{-1}g-(\gamma-1)\,g\,dL/dT}\right]\frac{p}{\rho}. \tag{7.7}$$

Although it is important to understand the conditions under which choking will occur upstream of the equilibrium state, surprisingly little analytical work appears to have been done on this problem. Most standard treatments use the classical shock equations ($H \gg 1$) to obtain an upper bound on the mass fraction (heat addition) but do this independently of the saturation constraint. A discussion of the choking and saturation conditions is given in appendix C for flows in which the latent heat is constant. Using this assumption ($\bar{L} = 1$) it is possible to obtain explicit solutions of the conservation relations in terms of the mass fraction $\bar{g}$. The analysis below is restricted to this case. These solutions can be written

$$\frac{\bar{u}}{u_k} = \frac{\rho_k}{\bar{\rho}} = \frac{\gamma M_k^2+1\pm\{\mathscr{D}(\bar{g}T_0^{-1}; M_k, HT_0^{-1}, \gamma)\}^{\frac{1}{2}}}{M_k^2[\gamma+1+(\gamma-1)\,\bar{g}H^{-1}]}, \tag{7.8}$$

where
$$\mathscr{D} = (M_k^2-1)^2 - 2\gamma^{-1}(\gamma-1)\,M_k^2 T_0 T_k^{-1} C(\bar{g}\bar{T}_k^{-1}; HT_0^{-1}, \gamma) \tag{7.9}$$

and
$$C = C_1\left(\frac{H}{T_0}, \gamma\right)\frac{\bar{g}}{T_0} - C_2\left(\frac{H}{T_0}, \gamma\right)\left(\frac{\bar{g}}{T_0}\right)^2 - C_3\left(\frac{H}{T_0}, \gamma\right)\left(\frac{\bar{g}}{T_0}\right)^3. \tag{7.10}$$

Here
$$C_1 = (\gamma+1) - \frac{2\gamma}{\gamma-1}\frac{T_0}{H}, \quad C_2 = \left(1+\gamma\frac{T_0}{H}\right)\frac{T_0}{H}, \quad C_3 = (\gamma-1)\left(\frac{T_0}{H}\right)^2, \tag{7.11}$$

and
$$T_0 = [1+\tfrac{1}{2}(\gamma-1)\,M_k^2]\,T_k = 1+\tfrac{1}{2}(\gamma-1)\,M_c^2. \tag{7.12}$$

Further
$$\frac{\bar{p}}{p_k} = 1+\gamma M_k^2\left[1-\frac{\bar{u}}{u_k}\right], \quad \frac{\bar{T}}{T_k} = \frac{\bar{p}}{p_k}\frac{\bar{u}}{u_k}\left(1-\frac{\bar{g}}{H}\right)^{-1} \tag{7.13}$$

Initially $\mathscr{D} > 0$. Choking corresponds to $\mathscr{D} = 0$. It is shown in appendix C that a saturated equilibrium state is always achieved upstream of choking if

$$T_0 > \tfrac{1}{2}(\gamma+1), \tag{7.14a}$$

or, equivalently, if
$$M_c > 1. \tag{7.14b}$$

Conversely, choked flows will arise only for

$$M_c < 1 \quad (T_0 < \tfrac{1}{2}(\gamma+1)). \tag{7.15}$$

This criterion does not appear to have been previously deduced by analytical arguments but it is implicit in some experimental studies of choking phenomena (see Pouring 1965). It should be stressed that (7.15) is a necessary rather than a sufficient condition. Choking will occur only for $M_c < 1$ and $M_k - 1$ sufficiently small. (In the preceding discussion $M_k > 1$.) Some detailed numerical calculations are presented in figures 8–10. For given H and γ these figures show the locus of the choking and equilibrium points in the $\bar{g}, \bar{T}$ plane for a pure vapour.

As implied above, the shock relations simplify considerably for $H \gg 1$ and reduce to the classical Rayleigh-line relations. In particular

$$C \to (\gamma+1)\,\bar{g}T_0^{-1} \quad \text{as} \quad H \to \infty. \tag{7.16}$$

However, it is easily seen from (7.10) and (7.11) that difficulties arise with the large H approximation when $T_0 = O(H)$, for which $M_k > M_c \gg 1$. It should also

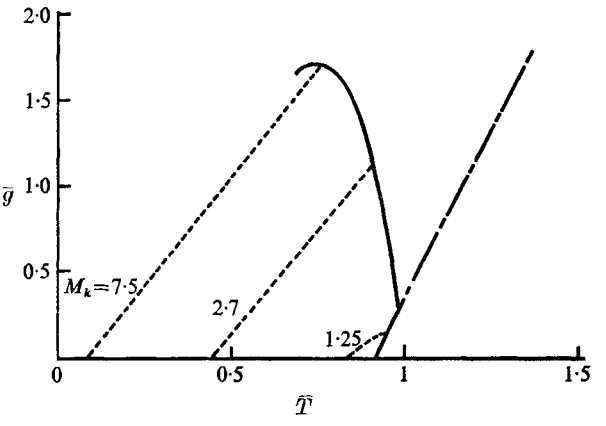

FIGURE 8. The shock solution for $T_0 < \frac{1}{2}(\gamma+1)$. Choking is possible for sufficiently small M_k. Shock paths originate on $\bar{g} = 0$. $T_0 = 1{\cdot}1$, $\omega_0 = 1$, $\gamma = 1{\cdot}4$, $H = 20$. – – – –, shock path; ——, local saturation limit; – — –, choking line.

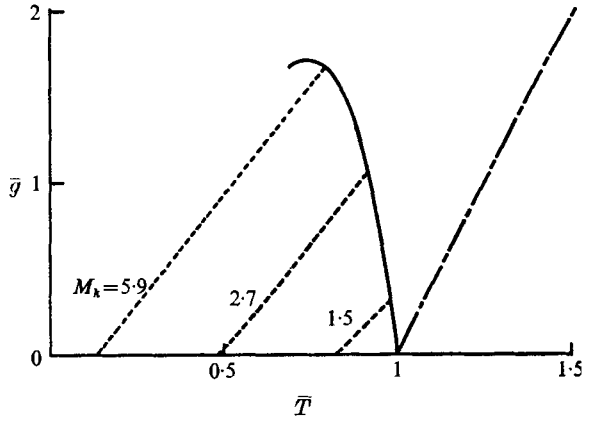

FIGURE 9. The shock solution for $T_0 = \frac{1}{2}(\gamma+1)$. The choking and saturation curves intersect only for $M_k = 1$ ($\bar{g} = 0$, $\bar{T} = 1$). Shock paths originate on $\bar{g} = 0$. $T_0 = 1{\cdot}2$, $\omega_0 = 1$, $\gamma = 1{\cdot}4$, $H = 20$. – – – –, shock path; ——, local saturation limit; – — –, choking line.

be noted from (7.11) that for T_0 sufficiently large $C_1 < 0$. In this case it follows from (7.10) that $C < 0$ and, irrespective of the saturation constraint, the flow will not choke for any value of $\bar{g}$.

If choking does occur, which requires at least that $C_1 > 0$, the cubic defined by $\mathscr{D} = 0$ has two positive roots for the limiting value of the mass fraction. The analysis given here considered only the smaller of these two roots. It is not clear whether the larger root corresponds to any real physical situation.

As the onset point moves towards the initial saturation point, the shock strength decreases. Flows in which $x_k - x_c = o(1)$ arise, at fixed K, for sufficiently large values of the growth parameter λ. It is necessary that

$$K \ln(\lambda/K) \gg 1. \tag{7.17}$$

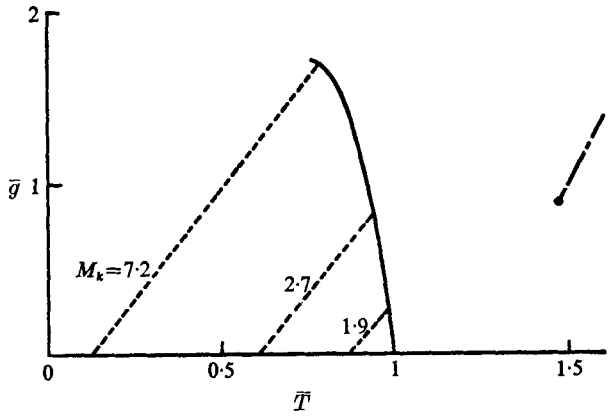

FIGURE 10. The shock solution for $T_0 > \frac{1}{2}(\gamma+1)$. The initial point on the choking line is defined by $\bar{T}_k = 1$ ($M_k > 1$). Shock paths originate on $\bar{g} = 0$. $T_0 = 1{\cdot}5$, $\omega_0 = 1$, $\gamma = 1{\cdot}4$, $H = 20$. – – – –, shock path; ——, local saturation limit; – — –, choking line.

If, however, $K \ll 1$ the structure of the nucleation zone is still governed by the analysis described in §5. (Even if K is not small the theory remains valid for $\lambda \gg K$.) From (4.5) it follows that the width of the nucleation zone is now $O[K(x_k - x_c)^2]$.

Downstream of this zone the solution corresponds to a weak condensation shock. Retaining only the dominant terms it can be shown that, as $x_k \to x_c$,

$$\bar{\Omega} \sim 1 - \beta\bar{g}, \tag{7.18}$$

where

$$(\gamma - 1 - H^{-1}\gamma)\, M_c^2 (dA/dx)_c (x_k - x_c)\beta = (\gamma-1)(M_c^2 - \gamma^{-1}) - 2H^{-1}(\gamma-1)M_c^2 + H^{-2}\{\gamma M_c^2 + \omega_0^{-1}(1-\omega_0)\mu_i^{-1}\mu_v(M_c^2-1)\}. \tag{7.19}$$

Suitable local dependent and independent variables can be defined by

$$\bar{g} = \beta^{-1}\bar{g}_w, \quad \bar{T} = b_{Tc}\beta^{-1}\bar{T}_w, \quad \bar{S} = \beta^{-\frac{1}{3}}\bar{S}_w \tag{7.20}$$

and

$$\chi = \beta^{-\frac{1}{3}}\chi_w. \tag{7.21}$$

Here b_{Tc} is given by (5.10) with M_k replaced by M_c, etc. In terms of these variables, omitting the suffix w, (6.21) reduces to

$$d\bar{S}/d\chi = 1 - \bar{S}^3 \tag{7.22}$$

with

$$\bar{g} = \bar{T} = \bar{S}^3. \tag{7.23}$$

Subject to the initial condition $S(0) = 0$, the solution of (7.22) can be written

$$\chi = \frac{1}{6}\ln\left[\frac{1+\bar{S}+\bar{S}^2}{(1-\bar{S})^2}\right] + \frac{1}{\sqrt{3}}\tan^{-1}\left[\frac{3^{\frac{1}{2}}\bar{S}}{\bar{S}+2}\right]. \tag{7.24}$$

This function, with $\bar{g} = \bar{S}^3$, is shown in figure 11.

It was assumed earlier that onset occurred downstream of the frozen sonic point although no assumptions were made concerning the position of x_c. As

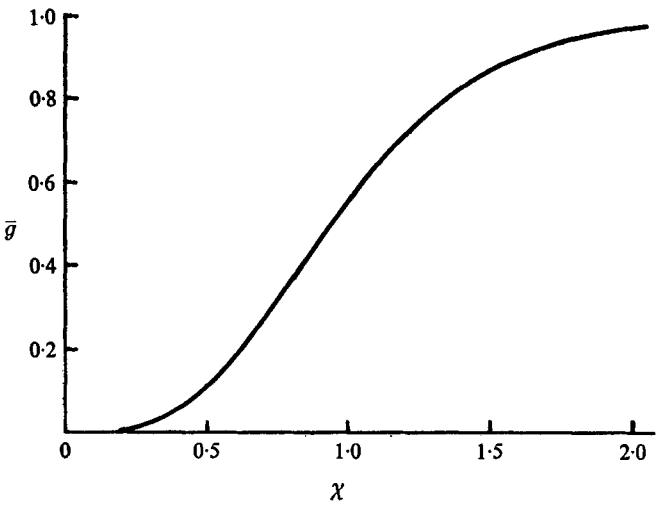

FIGURE 11. Weak shock structure.

$x_k \to x_c$ it is clearly desirable, if subsonic saturation points are to be permitted, to remove this limitation. Provided that the mass flow is redefined by its equilibrium value, it is not difficult to show that the weak shock analysis is also valid for $u_c < a_{ec}$, where a_e is the saturated equilibrium sound speed. The analysis is not valid in the transonic regime

$$a_{fc} \geqslant u_c \geqslant a_{ec}, \tag{7.25}$$

where $\beta \leqslant 0$. Similar comments apply to the general case, $x_k - x_c = O(1)$. Many of the results derived earlier will remain valid for $u_k < a_{ec}$ if the mass flow is suitably modified and if $b > 0$ [see (5.9)].

From (7.23) it can be seen that figure 11 also defines the temperature distribution for weak shocks. Outside the interval (7.25), $b_{Tc} > 0$ except for

$$a_{ec}' > u_c > a_{Tc}, \tag{7.26}$$

where a_T is the isothermal sound speed. Within this latter range it appears from (7.20) that the heat release due to condensation will decrease the local temperature (Shapiro 1953). Although, in addition, $b_{Tc} < 0$ over the transonic range (7.25), no conclusions should be drawn for that interval since the present theory is not applicable.

8. Collapse structure, $x_m - x_k = o(1)$

In §§5–7 it was assumed that the onset point did not lie close to the frozen turning point x_m (see figure 3). From (4.9) the structure of the onset region must be modified when

$$x_m - x_k = O(K^{\frac{1}{2}}). \tag{8.1}$$

Consistent with (8.1), it is then convenient to introduce the variable

$$\zeta_1 = K^{-\frac{1}{2}}(x - x_m). \tag{8.2}$$

The initial growth law (4.4), neglecting the error term $O(g/K)$, becomes

$$g \sim \lambda^3 K^2 \Omega_m^3 \Sigma_m A_m \exp\{-K^{-1}B_m\} \int_{-\infty}^{\zeta_1} (\zeta_1 - z_1)^3 \exp[-\tfrac{1}{2}B_m'' z_1^2]\, dz_1 [1 + O(K^{\frac{1}{2}})], \tag{8.3}$$

where
$$B_m = B_f(x_m), \quad B_m'' = (d^2 B_f/dx^2)_m, \tag{8.4}$$
etc.

Corresponding to the definition (4.10), it is appropriate to write

$$D_m = \lambda^3 K \Omega_m^3 \Sigma_m A_m \exp\{-K^{-1}B_m\}. \tag{8.5}$$

For the analysis given earlier, with $B_f' = O(1)$, $D_m \gg 1$. Here $B_f' = O(K^{\frac{1}{2}})$ and $D_m = O(1)$. Even though $|x_k - x_m| = o(1)$, the restriction $D_m = O(1)$ still implies that $\lambda \gg 1$. From (8.5) and (8.3) the initial growth is apparently given by

$$g \sim K D_m \int_{-\infty}^{\zeta_1} (\zeta_1 - z_1)^3 \exp\{-\tfrac{1}{2}B_m'' z_1^2\}\, dz_1, \tag{8.6}$$

but clearly the error term $O(g/K)$ [see (4.4)] cannot be neglected for finite ζ_1. Equation (8.6) is valid only as $\zeta_1 \to -\infty$.

The correct expansion for $\zeta_1 = O(1)$ has the form

$$\left.\begin{aligned} g(x;K) &= \mathscr{G}(\zeta_1;K) = K\mathscr{G}_2(\zeta_1) + \ldots, \\ T(x;K) &= \mathscr{T}(\zeta_1;K) = T_m + K^{\frac{1}{2}}\mathscr{T}_1(\zeta_1) + K\mathscr{T}_2(\zeta_1) + \ldots, \end{aligned}\right\} \tag{8.7}$$

with similar results for the remaining dependent variables. Again $T_m = T_f(x_m)$, etc. It is easily shown that the terms $O(K^{\frac{1}{2}})$ are defined by the frozen solution ($g \equiv 0$); any departure from the supersaturated state is associated with the terms $O(K)$. In particular, it follows from the conservation equations (§2) that

$$(M_m^2 - 1)\mathscr{T}_2 = \tfrac{1}{2}(M_m^2 - 1)T_m'' \zeta_1^2 + (\gamma - 1)[M_m^2 - \gamma^{-1} - H_m^{-1}M_m^2] L_m G_2. \tag{8.8}$$

Equation (8.8) should be compared with (5.4), which holds when $D_m \gg 1$.

Substitution in the rate equation (3.9) gives

$$\hat{\mathscr{G}}(\zeta;\nu) = \nu \int_{-\infty}^{\zeta} (\zeta - z)^3 \exp[-z^2 - \hat{\mathscr{G}}(z;\nu)]\, dz, \tag{8.9}$$

where
$$\hat{\mathscr{G}} = b\mathscr{G}_2, \quad \zeta = (\tfrac{1}{2}B_m'')^{\frac{1}{2}}\zeta_1 \tag{8.10}$$

and
$$\nu = 4b(B_m'')^{-2} D_m. \tag{8.11}$$

In contrast with (5.14), which is valid for $D_m \gg 1$, the reduced nucleation equation now does depend on the single parameter ν.

Solutions for the droplet production rate

$$\hat{J}(\zeta;\nu) = \exp[-\zeta^2 - \hat{\mathscr{G}}(\zeta;\nu)], \tag{8.12}$$

for the normalized droplet number density

$$\hat{N}(\zeta;\nu) = \int_{-\infty}^{\zeta} \hat{J}(z;\nu)\, dz, \tag{8.13}$$

and for the asymptotic level $\hat{N}(\infty;\nu)$, which is proportional to the total number

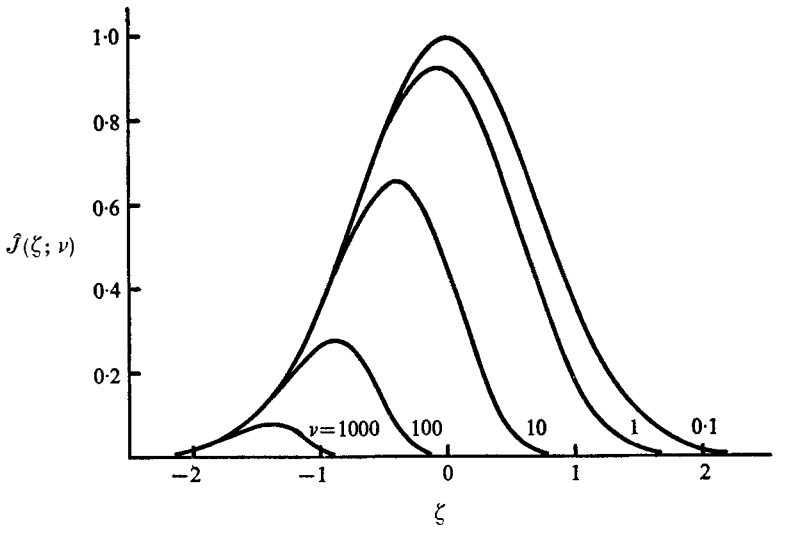

FIGURE 12. The droplet production rate, $x_m - x_k = o(1)$.

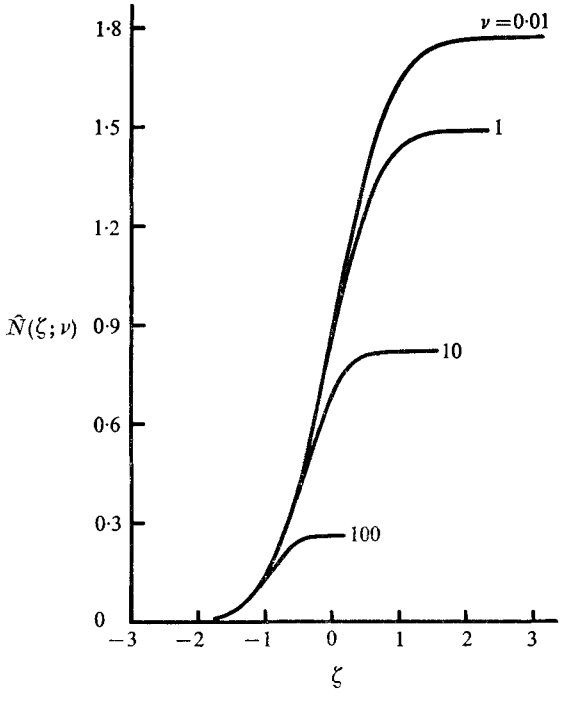

FIGURE 13. Droplet number density, $x_m - x_k = o(1)$.

of nuclei produced, are shown in figures 12–14. The solution for the mass fraction $\hat{\mathscr{G}}(\zeta;\nu)$ is given in figure 15. From (8.9) it follows that as $\zeta \to \infty$ the mass fraction is again governed by a cubic law

$$\hat{\mathscr{G}}(\zeta;\nu) \sim \alpha_3(\nu)\,\zeta^3 + \ldots + \alpha_0(\nu) + o(1), \tag{8.14}$$

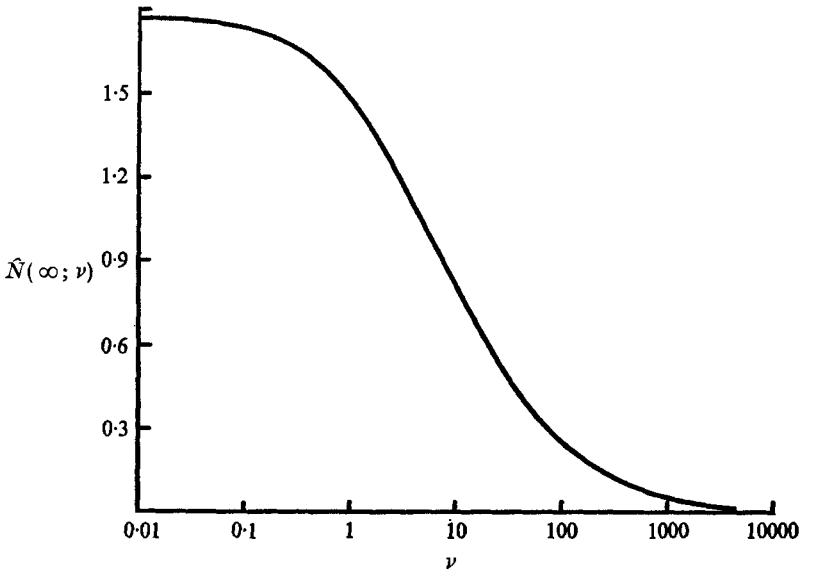

FIGURE 14. The asymptotic droplet number, $x_m - x_k = o(1)$.

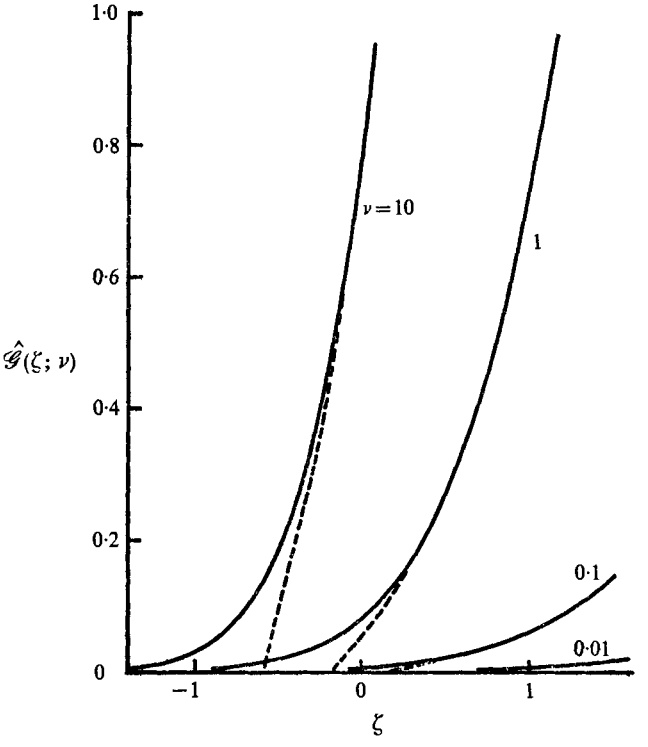

FIGURE 15. Condensate mass fraction, $x_m - x_k = o(1)$.
– – – –, asymptotic solution (8.14).

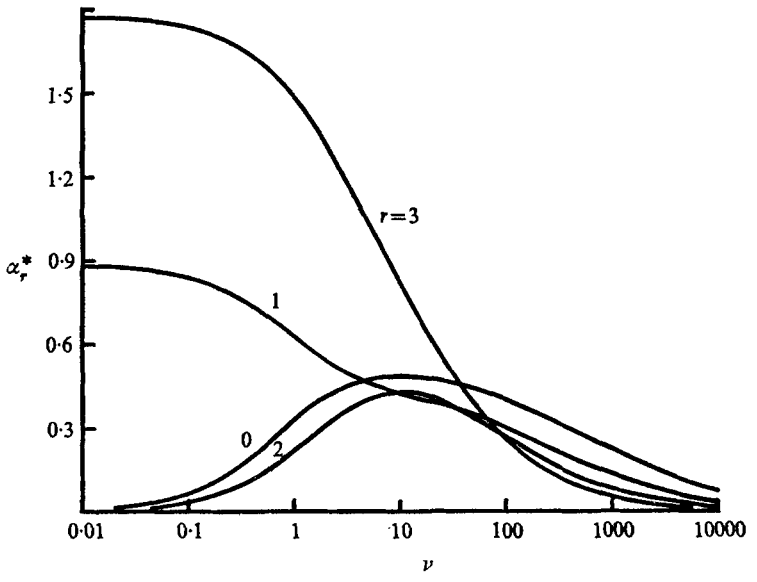

FIGURE 16. The coefficients $\alpha_r(\nu)$. $\alpha_r^* = \nu^{-1}\alpha_r/C_r$.

with
$$\alpha_r(\nu) = {}_3C_r\,\nu\int_{-\infty}^{\infty}(-\zeta)^{3-r}\exp[-\zeta^2-\hat{\mathscr{G}}(\zeta;\nu)]\,d\zeta. \tag{8.15}$$

Note that
$$\hat{N}(\infty;\nu) = \nu^{-1}\alpha_3(\nu). \tag{8.16}$$

The coefficients $\alpha_r(\nu)$ are shown in figure 16.

As in § 5, the growth defined by (8.14) cannot persist indefinitely. This solution fails when $g = O(1)$ or, from (8.2) and (8.14), when

$$x - x_m = O(K^{\frac{1}{3}}). \tag{8.17}$$

Within this latter zone the dominant approximation is governed by the shock relations discussed in § 7. Here, however, the error term due to the area variation is $O(K^{\frac{1}{3}})$.

Similar results to those outlined in § 6 can be obtained for the shock structure. In terms of
$$\tilde{\chi} = (b^{-1}\alpha_3)^{\frac{1}{3}}(\tfrac{1}{2}B_m'')^{\frac{1}{2}}K^{-\frac{1}{3}}(x-x_m), \tag{8.18}$$

the dependent variables have expansions

$$g(x;K) = \tilde{g}(\tilde{\chi};K) = \tilde{g}(\tilde{\chi}) + O(K^{\frac{1}{3}}), \tag{8.19}$$

etc. The constant factor in (8.18) is introduced for algebraic convenience. It follows that the growth law reduces to

$$d\tilde{S}/d\tilde{\chi} = \tilde{\Omega}(\tilde{S}), \tag{8.20}$$

where
$$\tilde{g} = \tilde{S}^3, \tag{8.21}$$

and
$$\tilde{\Omega} = \Omega_m^{-1}\Omega(x;K) \tag{8.22}$$

is evaluated as a function of $\tilde{g}(\tilde{S})$ from the shock relations. Matching with the

nucleation solution implies that

$$\tilde{\chi} = \int_0^{\tilde{S}} \frac{d\sigma}{\tilde{\Omega}(\sigma)}, \tag{8.23}$$

where the error term, which corresponds to the shock thickness or area variation, is $O(K^{\frac{1}{3}})$. Since, at fixed K, $x_k \to x_m$ as λ decreases this increase in shock thickness could have been expected.

9. Weak coupling, $D_m = o(1)$

The growth laws discussed in § 8 for $D_m = O(1)$ do not necessarily remain valid as $D_m \to 0$. Flows in which $D_m = o(1)$ arise, at fixed K, as λ decreases. From (8.6) it can be seen that $g = O(KD_m)$ in the nucleation zone and, if $D_m = o(1)$, the coupling term $O(g/K)$ remains small throughout this region. Droplet production is then governed entirely by the frozen approximation ($g \equiv 0$) to the nucleation rate J. In this limit, which corresponds to $\nu \to 0$, (8.6) implies that

$$g \sim 4\pi^{\frac{1}{2}}(B_m'')^{-2} KD_m[\zeta^3 + 2\zeta + o(1)] \tag{9.1}$$

as $\zeta \to \infty$. The validity of (9.1) is limited either by droplet growth or by the local area increase. As before, droplet growth is important when $g = O(1)$, which, from (9.1), occurs when

$$\zeta = O(KD_m)^{-\frac{1}{3}}, \tag{9.2}$$

or equivalently, from (8.2), when

$$x - x_m = O(K^{\frac{1}{3}} D_m^{-\frac{1}{2}}). \tag{9.3}$$

Apparently the area variation will remain small if

$$KD_m^{-2} = o(1). \tag{9.4}$$

Downstream of x_m the nucleation rate is exponentially small. Using arguments similar to those given in § 6, the local growth law can be written as

$$dR/dx = \Omega/\Omega_m, \tag{9.5}$$

where

$$g = (2\pi)^{\frac{1}{2}} (B_m'' K)^{-\frac{1}{2}} D_m R^3, \tag{9.6}$$

and $R = 0$ on $x = x_m$. Only the dominant terms are retained in (9.5) and (9.6). The constant factor in (9.6) follows from matching with the nucleation solution (9.1). If the restriction (9.5) holds, a suitable local length scale, downstream of x_m, is defined by

$$x - x_m = (2\pi)^{-\frac{1}{6}} (B_m'' K)^{\frac{1}{6}} D_m^{-\frac{1}{3}} \tilde{\chi}, \tag{9.7}$$

with

$$R = (2\pi)^{-\frac{1}{6}} (B_m'' K)^{\frac{1}{6}} D_m^{-\frac{1}{3}} \tilde{S}. \tag{9.8}$$

This scaling corresponds to the $\nu = 0$ limit of the transformation given in § 8. $\tilde{S}$ again satisfies (8.20) with $\tilde{\Omega}$ defined by the one-dimensional shock relations. Here, however, the shock thickness is $O(K^{\frac{1}{3}} D_m^{-\frac{1}{3}})$ and the collapse is considerably more diffuse.

For even smaller values of D_m, such that

$$D_m K^{-\frac{1}{2}} = O(1), \tag{9.9}$$

it is apparent from (9.3) that the validity of the growth law (9.1) will also be limited by the area variation. Equations (9.5) and (9.6) still hold downstream of x_m, but now g, R and $x-x_m$ are all $O(1)$ and Ω must be evaluated using the full conservation equations including the local area variation. In this limit, with $D_m = O(K^{\frac{1}{2}})$, the collapse of the supersaturated state is no longer shock-like.

Finally, as λ decreases further, flows in which $D_m = o(K^{\frac{1}{2}})$ can be obtained. Equations (9.5) and (9.6) then imply that g will remain small for $x-x_m = O(1)$. Droplet growth, even downstream of x_m, can be computed from the frozen approximation to Ω. This near-frozen behaviour may ultimately collapse, as $x \to \infty$, depending on the form of the growth function and on the asymptotic nozzle shape. No discussion of this limit is given here but related problems have been discussed in Blythe (1967) and Petty (1968).

10. Discussion

In flows with $K \ll 1$ it can be expected that significant nucleation will not occur for some distance downstream of the initial saturation point x_c. If, further, $\lambda \gg 1$ it can also be expected that any subsequent growth will be rapid. These conditions, $K \ll 1$ and $\lambda \gg 1$, are certainly necessary for the existence of condensation shocks, but they are by no means sufficient. It was however shown in §7 that, if the onset occurs upstream of x_m, then the eventual collapse is governed by a condensation shock. The end state downstream of the shock corresponds to saturation if the flow is supersonic at x_c: choking is possible only for $M_c < 1$.

It was found that the collapse of the supersaturated region was, in general, governed by a two-layer structure in which the nucleation zone (§5) acts as a precursor for the subsequent growth or shock zone. Within the shock zone droplet production is exponentially small. Of particular interest, with respect to the collapse structure, is the solution in the nucleation zone. When x_k does not lie close to x_m, it was shown in §5 that the governing integral equation can be reduced to a parameter-free form. Further, even as $x_k \to x_m$, it was noted in §8 that the corresponding integral equation still depends only on the single parameter ν. Although no attempt is made in the present paper it would certainly be of interest to use the transformations discussed in §§5 and 8 to analyse available data for the nucleation rate J. Possibly, because of uncertainties in the experimental results, the simplest way of testing these scaling laws would be to use numerical solutions of the full equations.

As λ decreases, at fixed K, $x_k \to x_m$. The analysis given in §§8 and 9 shows that the shock zone broadens significantly in this limit and, even though $\lambda \gg 1$, the collapse is no longer shock-like when

$$\lambda = O(K^{-\frac{1}{6}} \exp\{\tfrac{1}{3}K^{-1}B_m\}) \tag{10.1}$$

[see (8.5) and (9.9)]. A corresponding trend, as the collapse moves downstream, is clearly evident in both experimental data and numerical solutions (Hill 1966). Table 2 summarizes the principal results for the collapse structure.

For very large values of the growth parameter λ the collapse point x_k will move towards the initial saturation point x_c. If $K \ll 1$ the collapse remains shock-

Onset point	λ	D_m	Width of nucleation zone	Width of growth zone	Comments
$x_m - x_k = O(1)$	$O(K^{-1}\exp\{\frac{1}{3}K^{-1}B_k\})$	$\gg 1$	$O(K)$	$O(K^{\frac{2}{3}})$	Shock
$x_m - x_k = O(K^{\frac{1}{2}})$	$O(K^{-\frac{1}{3}}\exp\{\frac{1}{3}K^{-1}B_m\})$	$O(1)$	$O(K^{\frac{1}{2}})$	$O(K^{\frac{1}{6}})$	Shock
$x_m - x_k = O(K^{\frac{1}{2}})$	$O(K^{-\frac{1}{6}}\exp\{\frac{1}{3}K^{-1}B_m\})$	$O(K^{\frac{1}{2}})$	$O(K^{\frac{1}{2}})$	$O(1)$	Diffuse

TABLE 2. Collapse structure

like, but the shock is now weak and the results for the structure simplify. In particular, the profile in the shock zone, as well as that in the nucleation zone, can be reduced to a similarity form (§7). The collapse will also occur close to x_c, for $\lambda \gg 1$, when K is not small. In this case the collapse is not necessarily shock-like and the local area variation can be important. This type of solution is described by Petty (1968).

The authors would like to acknowledge the help and advice they received from Prof. J. F. Clarke, Dr J. P. Hodgson and Prof. N. H. Johannesen. Some of the results presented in this paper were obtained in the course of research sponsored by Department of Defense project THEMIS under contract no. DAAD05-69-C-0053 and monitored by the Ballistics Research Laboratories, Aberdeen Proving Ground, Md. The work was completed while one of us (P.A.B) held a Visiting Professorship at the University of Newcastle-upon-Tyne.

Appendix A. Normalized variables

Apart from the mass fraction g', all primed variables have dimensions. Dependent variables are normalized with respect to their values at the initial saturation point ($T = T'/T'_c$, etc.) except that

$$u = u'(\mu_0/\mathscr{R}T'_c)^{\frac{1}{2}}, \quad g = (\mu_0/\mu_v)Hg'. \tag{A 1}$$

In (A 1)
$$H = \mu_v L'_c/\mathscr{R}T'_c, \tag{A 2}$$

and $\mathscr{R}$ is the gas constant. Since it is assumed that the initial isentrope crosses the co-existence line
$$H > c_{p0} = \gamma/(\gamma-1) = \mu_0 c'_{p0}/\mathscr{R}. \tag{A 3}$$

The non-dimensional pressure p is related to the partial pressures p_v and p_i, of the vapour and carrier gas respectively, by

$$p = (1-\omega_0)\mu_0\mu_i^{-1}p_i + \omega_0\mu_0\mu_v^{-1}p_v \tag{A 4}$$

with
$$p_v = \frac{\mu_0\omega_0 H - \mu_v g}{\mu_0\omega_0(H-g)}p, \tag{A 5}$$

where ω_0 is the reservoir specific humidity (ratio of vapour mass to total mass). Obviously, for the molecular weights,

$$\mu_0^{-1} = (1-\omega_0)\mu_i^{-1} + \omega_0\mu_v^{-1}. \tag{A 6}$$

Similarly
$$\rho_v = [1 - H^{-1}\omega_0^{-1}\mu_0^{-1}\mu_v g]\rho, \tag{A 7}$$

where ρ_v is the normalized vapour density. In dimensional variables

$$\rho' = \rho'_i + \rho'_v + \rho'_l, \tag{A 8}$$

where ρ'_l is the density of the condensate defined with respect to the volume occupied by the carrier gas and the vapour. Using these results it is straightforward to show, treating the vapour phase of each component as a perfect gas, that the equation of state for the mixture reduces to (2.7).

For the growth law (3.5) and the rate equation (3.9) the appropriate normalization is given by

$$x = x'/h'_t, \quad F = F'/F'_c, \quad \lambda = (h'_t/r'_d)\,F'_c T'_c, \quad r = r'/r'_d, \tag{A 9}$$

where h'_t is the nozzle throat height. The characteristic droplet radius r'_d is determined from

$$\frac{\frac{4}{3}\pi\rho'_{\text{cond}} r'^3_d S' A'_c h'_t}{m'} = \frac{\mu_v}{\mu_0 H}. \tag{A 10}$$

Here ρ'_{cond} is the true density of the condensed phase. Each side of (A 10) represents a characteristic mass fraction [see (3.6) and (A 1)].

Appendix B. Equilibrium flows

Equilibrium states of a saturated vapour are governed by the Clausius–Clapeyron equation (2.1). Using the conservation equations it is not difficult to show that the equilibrium solution, in non-dimensional form, is governed by

$$\frac{dg}{dT} = \frac{1}{T}\frac{(c_{p0}T - H + g)(\omega_0\mu_0 H - \mu_v g)}{\omega_0\mu_0(H-T) + \mu_v(T-g)}. \tag{B 1}$$

Equation (B 1) can be integrated to give

$$g - (1-\omega_0)\frac{\mu_0}{\mu_1} T \ln\left(1 - \frac{\mu_v}{\mu_0\omega_0}\frac{g}{H}\right) = H(1-T) + c_{p0} T \ln T. \tag{B 2}$$

For a pure vapour, $\omega_0 = 1$, (B 2) reduces to the known result

$$g = H(1-T) + c_{p0} T \ln T \tag{B 3}$$

(Buhler 1952). The general integral (B 2) was first given in Shih (1972).

Appendix C. The choking condition ($M_k > 1$)

As noted in § 7, choking is possible only if

$$C_1 = \gamma + 1 - \frac{2\gamma}{\gamma - 1}\frac{T_0}{H} > 0, \tag{C 1}$$

otherwise $\mathscr{D} > 0$ for all g. The maximum permissible heat addition is defined by $g' = \omega_0$ or

$$\bar{g} = \mu_0\mu_v^{-1}\omega_0 H \leqslant H. \tag{C 2}$$

On the supersonic branch of the shock relations, upstream of choking,

$$\infty > d\bar{T}/d\bar{g} > 0. \tag{C 3}$$

Initially, at x_k, $\bar{T} < \bar{T}_s$. If it can be established that

$$\bar{T}^* > \bar{T}_s^*, \tag{C 4}$$

where starred variables are evaluated at choking, at least one equilibrium point must have been attained upstream of choking.

From the shock relations

$$\bar{T}^* = \frac{2T_0}{\gamma+1} \frac{(\gamma M_k^2+1)^2}{(\gamma+1)\,M_k^2\left[1+\left(\frac{\gamma-1}{\gamma+1}\right)(M_k^2-1)\right]} \frac{1+(\gamma-1)\,\delta}{\left[1+\left(\frac{\gamma-1}{\gamma+1}\right)\delta\right]^2(1-\delta)} \tag{C 5}$$

and

$$\bar{p}_v^* = \left(\frac{2T_0}{\gamma+1}\right)^{\gamma/(\gamma-1)} \left(\frac{\gamma M_k^2+1}{\gamma+1}\right) \left[1+\left(\frac{\gamma-1}{\gamma+1}\right)(M_k^2-1)\right]^{\gamma/(\gamma-1)} \times \frac{[1+(\gamma-1)\,\delta]\,[1-\mu_v\mu_0^{-1}\omega_0\,\delta]}{\left[1+\left(\frac{\gamma-1}{\gamma+1}\right)\delta\right][1-\delta]}, \tag{C 6}$$

where

$$\delta = \bar{g}^*/H < 1. \tag{C 7}$$

Hence, for $M_k > 1$,

$$\bar{T}^* > \frac{2T_0}{\gamma+1} \frac{[1+(\gamma-1)\,\delta]}{\left[1+\left(\frac{\gamma-1}{\gamma+1}\right)\delta\right]^2[1-\delta]} = T_l^* \tag{C 8}$$

and

$$\bar{p}_v^* < \left(\frac{2T_0}{\gamma+1}\right)^{\gamma/(\gamma-1)}[1+(\gamma-1)\,\delta] = p_{vu}^*. \tag{C 9}$$

Apparently, from (2.9) with $\bar{L} = 1$, (C 4) will hold if

$$\exp[H(1-T_l^{*-1})] > p_{vu}^*. \tag{C 10}$$

The results (A 3), (C 1), (C 7), (C 8) and (C 9) can be used to establish (C 10) provided that further

$$T_0 > \tfrac{1}{2}(\gamma+1), \tag{C 11a}$$

or, equivalently,

$$M_c > 1. \tag{C 11b}$$

Consequently, the asymptotic limit of the shock solution will always correspond to a saturated equilibrium state for $M_c > 1$. Conversely, it is necessary, though not sufficient, that $M_c < 1$ for choking to occur.

REFERENCES

Andres, R. P. 1969 Homogeneous nucleation in a vapor. In *Nucleation* (ed. A. C. Zettlemoyer). Marcel Dekker.

Blythe, P. A. 1967 Near-frozen quasi-one-dimensional flow. II. *Phil. Trans.* A **262**, 225.

Buhler, R. D. 1952 Condensation of air components in hypersonic wind tunnels. Theoretical calculations and comparison with experiments. Ph.D. thesis, Caltech.

Clark, D. R. 1963 On the flow in a nozzle of a condensing diatomic vapour. *Cranfield Coll. Aero. Rep.* no. 165.

Daum, P. L. & Gyarmathy, G. 1968 Condensation of air and nitrogen in hypersonic wind tunnels. *A.I.A.A. J.* **6**, 458.

GRIFFIN, J. L. & SHERMAN, P. M. 1965 Computer analysis of condensation in highly expanded flows. *A.I.A.A. J.* **3**, 1813.

HILL, P. G. 1966 Condensation of water vapour during supersonic expansion in nozzles. *J. Fluid Mech.* **25**, 593.

HILL, P. G., WHITTING, H. & DEMETRI, E. P. 1963 Condensation of metal vapors during rapid expansion. *J. Heat Transfer*, **6**, 303.

LOTHE, J. & POUND, G. M. 1962 Reconsiderations of nucleation theory. *J. Chem. Phys.* **36**, 2080.

LUKASIEWICZ, J. & ROYLE, J. K. 1953 Effects of air humidity in supersonic wind tunnels. *Aero. Res. Counc. R. & M.* no. 2563.

OSWATITSCH, K. 1941 Die Nebelbildung in Windkanälen und ihr Einfluss auf Modellversuche. *Jahrbuch der Deutschen Luftfahrtforschung*, **1**, 703.

OSWATITSCH, K. 1942 Kondensationserscheinungen in Überschalldüsen. *Z. angew. Math. Mech.* **22**, 1.

PETTY, D. G. 1968 Some aspects of hypersonic nozzle flows. Ph.D. thesis, University of London.

POURING, A. A. 1965 Thermal choking and condensation in nozzles. *Phys. Fluids*, **8**, 1802.

SHAPIRO, A. H. 1953 *The Dynamics and Thermodynamics of Compressible Fluid Flow.* Ronald Press.

SHIH, C. J. 1972 Condensation effects in nozzle flows. Ph.D. thesis, Lehigh University.

STEVER, H. G. 1958 Condensation phenomena in high speed flows. In *Fundamentals of Gas Dynamics. High Speed Aerodynamics and Jet Propulsion*, vol. III. Princeton University Press.

VOLMER, M. 1939 *Kinetik der Phasenbildung.* Steinkopff.

WEGENER, P. P. 1969 Gas dynamics of expansion flows with condensation, and homogeneous nucleation of water vapor. In *Non-equilibrium Flows*, part 1, chap. 4. Marcel Dekker.

WEGENER, P. P. 1975 Nonequilibrium flow with condensation. *Acta Mechanica*, **21**, 65.

WEGENER, P. P., CLUMPNER, J. A. & WU, B. J. C. 1972 Homogeneous nucleation and growth of ethanol drops in supersonic flow. *Phys. Fluids*, **15**, 1869.

WEGENER, P. P. & MACK, L. M. 1958 Condensation in supersonic and hypersonic wind tunnels. In *Advances in Applied Mechanics*, vol. v. Academic.

WEGENER, P. P. & PARLANGE, J. Y. 1967 Non-equilibrium nozzle flow with condensation. *Recent Advances in Aerothermochemistry*, **2**, 607 (*Agard Conf. Proc.* no. 12).